	1	6	3	1	2036.72	1043.24	3	T7	V69-K78 (1106.62)	1042.78					
	1	5	4	1	2077.75	1057.08	3	T7	V69-K78 (1106.62)	1056.46					
	2	6	4	0	2094.76	1062.65	3	T6	V69-K78 (1106.62)	1062.13	1282.43	3	A7	D64-K78 (1766.01)	1281.93
	1	4	5	1	2118.77	1070.38	3	T7	V69-K78 (1106.62)	1070.14					
	2	5	5	0	2135.79	1076.32	3	T6	V69-K78 (1106.62)	1075.81					
	1	6	4	1	2239.80	1110.97	3	T7	V69-K78 (1106.62)	1110.48					
	3	5	5	0	2281.85	1124.78	3	T6	V69-K78 (1106.62)	1124.49					
	1	7	5	0	2313.84	851.76	4	T6	V69-K78 (1106.62)	851.62					
	1	4	6	1	2321.85	1138.16	3	T7	V69-K78 (1106.62)	1137.83					
	2	5	6	1	2629.96	1241.13	3	T7	V69-K78 (1106.62)	1240.53					
Asn98	0	5	2	0	1234.43	1168.34	2	T1	V89-K99 (1117.54)	1167.99	912.24	3	A2	E86-K99 (1515.76)	911.74
											1367.31	2	A2	E86-K99 (1515.76)	1367.10
											930.26	3	A3	Q92-R105 (1570.84)	930.10
											1021.28	3	A3	E86-N102 (1843.94)	1021.13
											1011.53	3	A4	T95-K110 (1815.06)	1010.81
											1516.43	2	A4	T95-K110 (1815.06)	1516.75
											1144.21	3	A5	E86-R105 (2212.18)	1143.88
	0	3	4	0	1316.49	1209.79	2	T1	V89-K99 (1117.54)	1209.02					
	0	3	5	0	1519.57	1310.68	2	T1	V89-K99 (1117.54)	1310.56	1007.10	3	A2	E86-K99 (1515.76)	1006.78
											1106.39	3	A4	T95-K110 (1815.06)	1106.55
											1239.21	3	A5	E86-R105 (2212.18)	1238.92
	2	3	4	0	1608.60						951.28	3	A4	G91-N102 (1259.61)	951.08
											1426.22	2	A4	G91-N102 (1259.61)	1426.11
	1	4	4	0	1624.60	951.37	3	T3	S96-D106 (1245.67)	951.76					
	0	5	4	0	1640.59	1371.84	2	T1	V89-K99 (1117.54)	1371.07	960.04	4	A5	E86-R105 (2212.18)	959.70
											1279.69	3	A5	E86-R105 (2212.18)	1279.26
	0	5	3	1	1728.61						1176.27	3	A4	T95-K110 (1815.06)	1176.23
	0	5	4	0	1640.59						1146.70	3	A4	T95-K110 (1815.06)	1146.89
	1	6	3	0	1745.62						1082.52	3	A2	E86-K99 (1515.76)	1082.13
											1181.80	3	A4	T95-K110 (1815.06)	1181.90
											986.38	4	A5	E86-R105 (2212.18)	985.96
											1314.72	3	A5	E86-R105 (2212.18)	1314.27
	1	5	4	0	1786.65						1195.47	3	A4	T95-K110 (1815.06)	1195.57
											996.54	4	A5	E86-R105 (2212.18)	996.21
											1328.49	3	A5	E86-R105 (2212.18)	1327.95
	1	5	3	1	1874.67						1018.89	4	A6	E86-R105 (2212.18)	1018.22
	0	6	3	1	1890.66	1496.18	2	T1	V89-K99 (1117.54)	1496.10	1230.24	3	A4	T95-K110 (1815.06)	1230.24
											1022.70	4	A6	E86-R105 (2212.18)	1022.22
	2	5	4	0	1932.71	1517.35	2	T1	V89-K99 (1117.54)	1517.13					
	1	6	4	0	1948.70	1525.78	2	T1	V89-K99 (1117.54)	1525.12	1150.13	3	A2	E86-K99 (1515.76)	1149.83
											1249.75	3	A4	T95-K110 (1815.06)	1249.59
											1259.45	3	A3	E86-N102 (1843.94)	1259.22
											1037.27	4	A5	E86-R105 (2212.18)	1036.73
											1382.34	3	A5	E86-R105 (2212.18)	1381.97
	1	6	3	1	2036.72						1059.07	4	A6	E86-R105 (2212.18)	1058.73
	0	6	4	1	2093.74						1298.06	3	A4	T95-K110 (1815.06)	1297.94
											1073.37	4	A6	E86-R105 (2212.18)	1072.99

[a] dHex, deoxyhexose; Hex, hexose; HexNAc, *N*-acetylhexosamine; NeuAc, *N*-acetylneuramic acid.

[b] Monoisotopic value.

[c] Theoretical peptide mass is indicated in parenthesis.

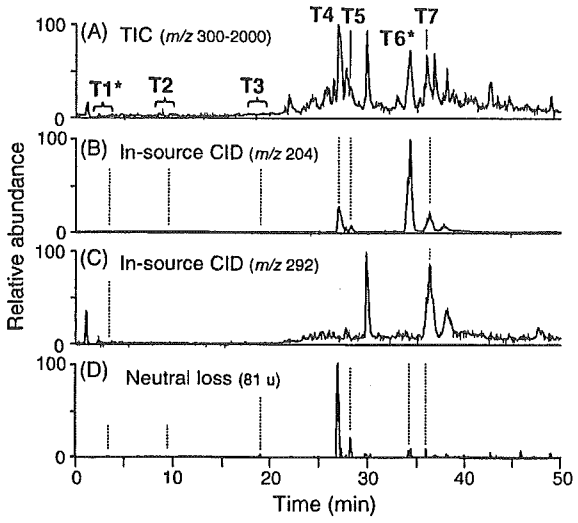

Fig. 2. Total ion chromatogram (TIC) of trypsin-digested protein at 20–25 kDa (*m/z* 300–2000) (A), mass chromatograms from TIC with ion-source CID of *m/z* 204 (B) and 292 (C), and neutral loss chromatogram of 81 u by data-dependent CID-MS/MS (D). Asterisks mean the peak of glycopeptides identified by the database search analysis.

the glycopeptide Val89-Lys99 contains two Asn residues, Asn93 and 98, only Asn98 was identified as a glycosylation site because of detection of b and y ions modified with GlcNAc at Asm98.

Next, to study the site-specific glycosylation at Asn74 and 98, product ion spectra of glycopeptides were sorted from the numbers of product ion spectra acquired around peak T6 and T1. We sorted out product ion spectra of glycopeptides using B series ions, such as $Hex_1HexNAc_1^+$ and $Hex_2HexNAc_1^+$ (*m/z* 366 and 528) originated from glycopeptides by CID-MS/MS, as marker ions [23]. We could sort out 14 product ion spectra originated from glycopeptide Val69-Lys78 around peak T6. The monosaccharide compositions of *N*-glycans at Val69-Lys78 were calculated as $dHex_{0-3}Hex_{2-7}HexNAc_{2-5}$ on the basis of the *m/z* values of their molecular ions and the theoretical mass of the peptide. Likewise, seven product ion spectra originated from glycopeptide Val89-Lys99 were sorted from those around peak T1, and their monosaccharide compositions were estimated as $dHex_{0-2}Hex_{3,5,6}HexNAc_{2-5}NeuAc_{0,1}$ (Table 1). Glycosylation at Asn74 and 98 were elucidated by a detailed examination of these product ion spectra as follows.

3.2.1. Analysis of the glycosylation at Asn74 of peptide Val69-Lys78

Fig. 3(A) shows a product ion spectrum of the glycopeptide Val69-Lys78 at 34.52 min. Its precursor ion is the doubly charged ion at *m/z* 1512.2. Many product ions generated by cleavages of glycosidic linkages can be observed in this product ion spectrum. The most intense ion at *m/z* 1311 is assigned to a peptide bearing the reducing end of GlcNAc, which was caused by glycosidic linkage cleavage of *N*-linked oligosaccharide. Fig. 3(B) is the product ion spectrum of the peptide + GlcNAc ion at *m/z* 1311. The b and y ions generated by cleavages of the peptide backbone prove that this glycopeptide is the peptide Val69-Lys78 glycosylated at Asn74.

The molecular weight of the carbohydrate moiety can be calculated as 1933.8 Da by subtracting the theoretical mass of the peptide (1106.6 Da) from the calculated glycopeptide mass (3022.4 Da). Consequently, the monosaccharide composition can be estimated as $dHex_2Hex_5HexNAc_4$. In the product ion spectrum (Fig. 3(A)), B ions corresponding to $dHex_1Hex_1HexNAc_1$ ($B_{2\alpha}$) and $dHex_1Hex_2HexNAc_1$ ($B_{3\alpha}$) were detected at *m/z* 512 and 674, respectively. These results indicate that one of two dHex, which are likely to be Fuc, attaches to Gal-GlcNAc at the non-reducing end in a similar manner as the Lewis a/x antigen (Gal-(Fuc-)GlcNAc-), or the blood group H-determinant (Fuc-Gal-GlcNAc-). The product ion at *m/z* 350 produced from the triply charged precursor ion at *m/z* 1008.7 corresponded to $dHex_1HexNAc_1$ (data not shown), suggesting that Fuc attaches to GlcNAc like the Lewis a/x antigen (Gal-(Fuc-)GlcNAc-). The attachment site of the other Fuc can be deduced at inner trimannosyl core GlcNAc from the observation of Y ions at *m/z* 1457, 1660, and 1822, which correspond to Val69-Lys78 plus $dHex_1HexNAc_1$ ($Y_{1\alpha}$), $dHex_1HexNAc_2$ ($Y_{2\alpha}$), and $dHex_1Hex_1HexNAc_2$ ($Y_{3\alpha/3\beta/3\gamma}$), respectively. In addition, the product ion at *m/z* 1411 resulting from the precursor ion at *m/z* 1512.2 by loss of 101.6 u (HexNAc), suggests a linkage of non-substituted HexNAc at the non-reducing terminal end. Together with detection of the product ion at *m/z* 940 ($Y_{3\alpha/1\beta/3\beta}^+$, [GlcNAc-Man-GlcNAc-GlcNAc-peptide+H]$^{2+}$), it can be deduced that this HexNAc is a bisecting GlcNAc attached to the core mannose residue via a β1–4 linkage. From these product ions, we could deduce two oligosaccharide structures. One is the structure indicated in Fig. 3(A), inset, and the other is one containing a Gal-Gal-(Fuc-)GlcNAc-Man-branch instead of a Gal-(Fuc-)GlcNAc-Man-branch. Detection of Gal-(Fuc-)GlcNAc-Man$^+$ at *m/z* 674 but not Gal-Gal-(Fuc-)GlcNAc-Man$^+$ at *m/z* 836 suggests that this oligosaccharide structure can be assigned to the structure indicated in Fig. 3(A), inset.

The carbohydrate structures of the other glycopeptide Val69-Lys78 detected around peak T6 can be characterized as the high-mannose-type oligosaccharide (M5), complex-type oligosaccharides containing some partial structures such as inner core Fuc, bisecting GlcNAc, the Lewis a/x antigen, and blood group H-determinant, and hybrid-type oligosaccharides (Table 1).

3.2.2. Analysis of the glycosylation at Asn98 of peptide Val89-Lys99

Fig. 4 shows one of the product ion spectra of the glycopeptide Val89-Lys99 at 3.47 min. Its precursor ion is the doubly charged ion at *m/z* 1525.8. The monosaccharide composition, $dHex_1Hex_6HexNAc_4$, can be estimated based on the calculated mass of the carbohydrate moiety (1950.0 Da) obtained by subtracting the mass of the theo-

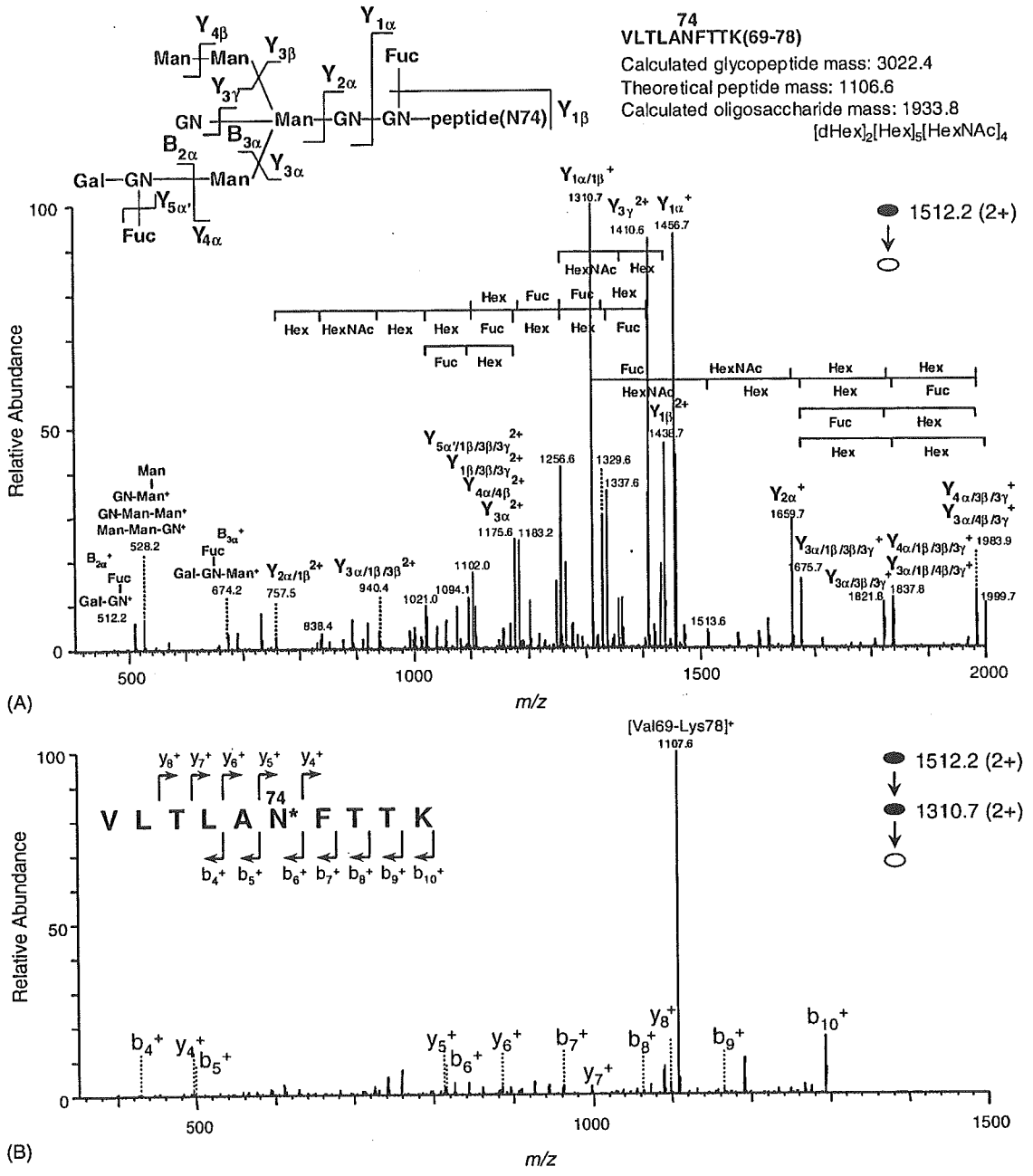

Fig. 3. (A) Product ion spectrum (MS^2) of the doubly charged glycopeptide precursor ion at *m/z* 1512.2 in peak T6. The glycopeptide Val69-Lys78 is glycosylated with oligosaccharide, $dHex_2Hex_5HexNAc_4$ at Asn74, and the inset is the deduced oligosaccharide structure. (B) MS^3 product ion spectrum derived from the doubly charged glycopeptide precursor ion at *m/z* 1512.2, followed by further fragmentation of the product ion at *m/z* 1310.7.

retical typtic peptide mass (1117.5 Da) from the calculated glycopeptide mass (3049.5 Da). Y ions corresponding to Val89-Lys99 plus $dHex_1HexNAc_1$ ($Y_{1\alpha}$), $dHex_1HexNAc_2$ ($Y_{2\alpha}$), and $dHex_1Hex_1HexNAc_2$ ($Y_{3\alpha/3\beta/3\gamma}$) detected at *m/z* 1468, 1671, and 1833, respectively, reveals that one Fuc residue is linked to the inner trimannosyl core GlcNAc. Additionally, the product ion at *m/z* 1424 suggests a linkage of non-substituted HexNAc at the non-reducing terminal end. Together with the product ions at *m/z* 945 and 1890, it can be deduced that this HexNAc is a bisecting GlcNAc that attaches to a core mannose residue via a β1–4 linkage. On the basis of the product ions at *m/z* 487, 528 and 1380, corresponding to Hex_3 ($B_{2\beta}$), $Hex_2HexNAc_1$ ($B_{3\alpha}$), and $Hex_6HexNAc_2$ ($B_{4\alpha}$), the oligosaccharide structure was characterized as a hybrid-type oligosaccharide (Fig. 4, inset).

The carbohydrate structures of the other glycopeptide Val89-Lys98 detected around peak T1 are characterized as high-mannose-type oligosaccharide (M5), complex-type, and hybrid-type oligosaccharides, which include bisecting GlcNAc and Lewis a/x structures (Table 1).

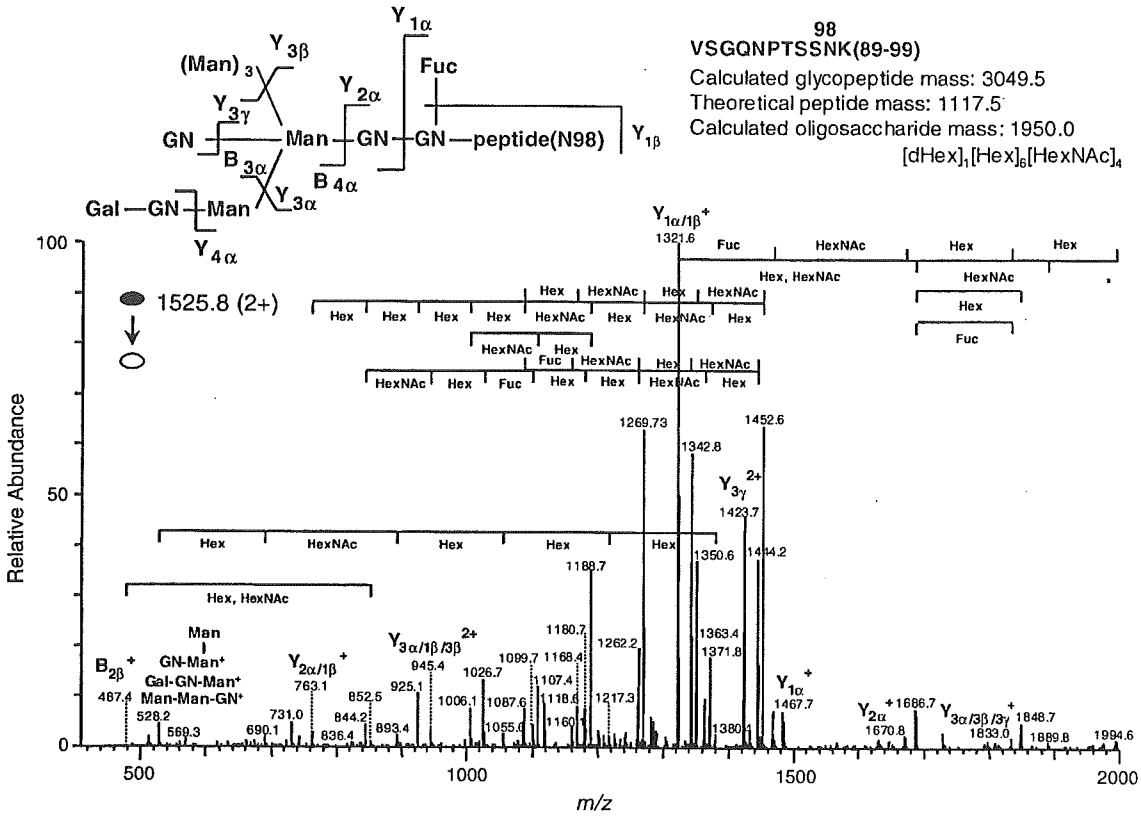

Fig. 4. Product ion spectrum of the doubly charged glycopeptide precursor ion at *m/z* 1525.8 in peak T1. The glycopeptide Val89-Lys99 is glycosylated with the oligosaccharide, $dHex_1Hex_6HexNAc_4$ at Asn98, and the inset is the deduced oligosaccharide structure.

3.3. Detection of glycopeptides by in-source CID and CID-MS/MS

Glycopeptides containing Asn23 could not be identified by the database search analysis. Therefore, we first localized all glycopeptides in the peptide/glycopeptide map using oxonium marker ions generated by in-source CID. Fig. 2(B and C) shows mass chromatograms of oxonium marker ions, $HexNAc^+$ (*m/z* 204) and $NeuAc^+$ (*m/z* 292), respectively. The mass chromatogram of *m/z* 204 indicates that the glycopeptides were localized around 3.7, 9.7, 19.1, 27.2, 28.4 34.3, 36.3, and 37.8 min. The mass chromatogram of *m/z* 292 suggests that the glycopeptides bearing NeuAc were localized around 3.7, 30.0, 36.4, and 38.2 min. In addition to the localization of glycopeptides by in-source CID, we monitored neutral loss caused by data-dependent CID-MS/MS. The neutral loss chromatogram of 81 u indicates the localization of doubly charged glycopeptides ions with Hex at the non-reducing ends. The elution positions of the localized glycopeptides by neutral loss are almost identical to those by in-source CID. Second, for confirmation of the elution position of glycopeptides and characterization of the carbohydrate moiety, we sorted the product ion spectra of glycopeptides from enormous numbers of data-dependently acquired product ion spectra around localized glycopeptides by using oligosaccharide oxonium ions as marker ions. Consequently, the locations of glycopeptides were confirmed in peak T1-6 (Fig. 2(A)). The peaks T1 and 6 correspond to the location of glycopeptides identified by the database search as Val89-Lys99 and Val69-Lys78, respectively. Four glycopeptide peaks were newly sorted by in-source CID and data-dependent CID-MS/MS. Structural assignment of the glycopeptides in these peaks was carried out using their MS^n spectra as follows.

3.3.1. Analysis of the glycosylation at Asn23 of peptide His21-Phe33

Fig. 5(A) shows one of the product ion spectra of the glycopeptide His21-Phe33 in peak T4. Its precursor ion is the triply charged ion at *m/z* 937.3. The intense product ion at *m/z* 899 is assigned to a doubly charged ion of peptide plus GlcNAc on the basis of Y series ions. The region of His21-Phe33 containing Asn23 in Thy-1 was suggested as the peptide moiety of this glycopeptide, 1593.3 Da, by the FindPept tool available on the internet (ExPASY Proteomics tools, Swiss Institute of Bioinformatics, http://us.expasy.org/tools/findpept.html). We examined the data-dependently acquired product ion spectrum of the precursor ion at *m/z* 899 and found that the *m/z* values of b and y ions in the product ion spectrum were identical to those of predictable product ions originating from the peptide His21-Phe33 modified with HexNAc at Asn23 (Fig. 5(B)). From the calculated oligosaccharide mass (1235.1 Da) obtained by subtracting the theoretical typtic

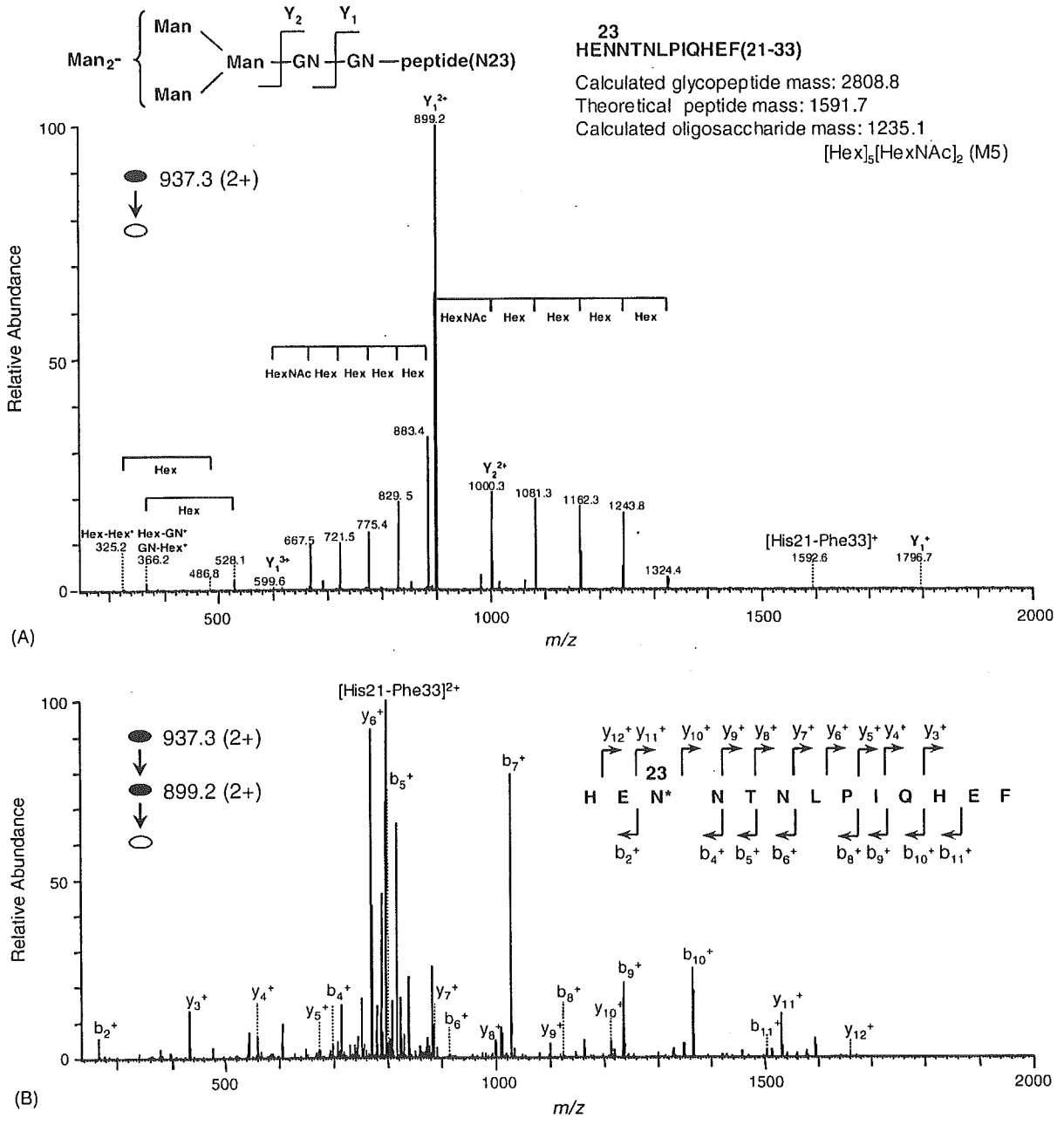

Fig. 5. (A) Product ion spectrum (MS^2) of the doubly charged glycopeptide precursor ion at *m/z* 937.3 in peak T4. The glycopeptide His21-Phe33 is glycosylated with oligosaccharide, $Hex_5HexNAc_2$ at Asn23, and the inset is the deduced oligosaccharide structure. (B) MS^3 product ion spectrum derived from a doubly charged glycopeptide precursor ion at *m/z* 937.3, followed by further fragmentation of the product ion at *m/z* 899.2.

peptide mass (1591.7 Da) from the calculated glycopeptide mass (2808.8 Da) together with product ions at *m/z* 366 and 528, it is indicated that this peptide carries $Hex_5HexNAc_2$, i.e. high-mannose-type oligosaccharide, M5. All product ion spectra in peak T4 revealed that peptides His21-Phe33 contain only high-mannose-type oligosaccharide (M5).

3.3.2. *Analysis of glycopeptides in peaks T2, 3, 5, and 7*

Similarly, product ion spectra of glycopeptides around peaks T2, 3, 5, and 7 were sorted by using oligosaccharide oxonium marker ions generated by MS/MS. In product ion spectra sorted out from around peak T2, the intense ion at *m/z* 884 was detected and assigned to a singly charged ion of a peptide plus GlcNAc. The peptide was suggested to be Ala73-Lys78 containing Asn74 by the FindPept tool. The monosaccharide composition can be estimated from the calculated mass of oligosaccharide moiety obtained by subtracting the theoretical mass of Ala73-Lys78 (680.35 Da) from calculated glycopeptide mass. Oligosaccharide structure of the glycopeptides is characterized based on their product

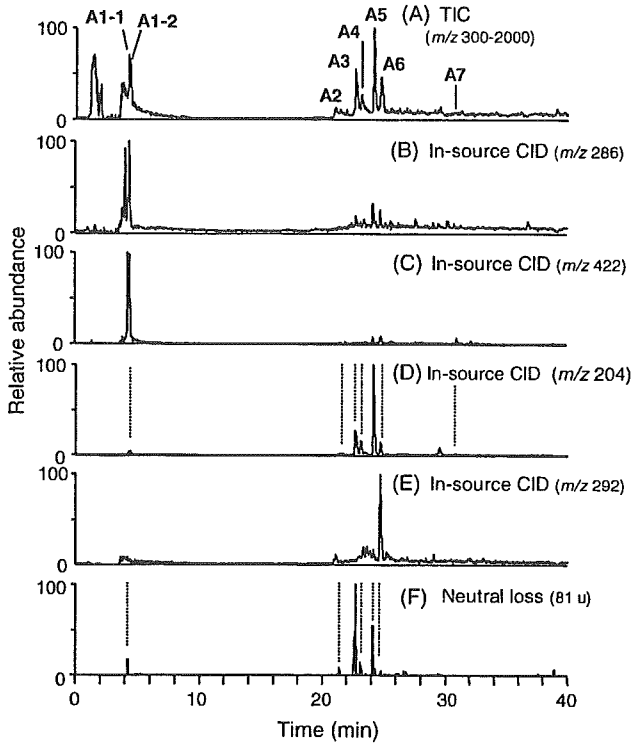

Fig. 6. Total ion chromatogram (TIC) of Asp-N digested protein at 20–25 kDa (*m/z* 300–2000) (A), mass chromatograms from TIC with ion-source CID of *m/z* 286 (B), 422 (C), 204 (D), and 292 (E), and neutral loss chromatogram of 81 u by data-dependent CID-MS/MS (F).

ion spectra. Glycopeptides in peak T2 were characterized as Ala73-Lys78 glycosylated at Asn74 with *N*-glycans consisting of $dHex_{0-2}Hex_{3-6}HexNAc_{2-5}$. These *N*-glycans can be identified as high-mannose-type oligosaccharide (M5), and complex-type and hybrid-type oligosaccharides containing Fuc attached to inner trimannosyl core GlcNAc. Their structural assignments are summarized in Table 1. Glycopeptides in peak T3 can be identified as a mixture of peptide His21-His31 and His21-Glu32 glycosylated at Asn23, and Ser96-Asp106 glycosylated at Asn98. Asn23 was attached by high-mannose-type oligosaccharides, M5, 6, and 7, and Asn98 was occupied by *N*-glycan consisting of $dHex_1Hex_4HexNAc_4$ with a Lewis a/x structure as a partial structure. Glycopeptides in peak T5 were characterized as peptide His21-Phe33 glycosylated at Asn23 with high-mannose-type oligosaccharide, M6. Glycopeptides in peak T7 were assigned to be Val69-Lys78 glycosylated at Asn74 with *N*-glycans composed of $dHex_{1-2}Hex_{4-6}HexNAc_{3-6}NeuAc$.

3.4. Analysis of the GPI moiety of rat Thy-1

Since trypsin digestion provided Cys-GPI, which could not be retained on the C_{18} column, Asp-N digestion was also performed to obtain more hydrophobic peptides attached by GPI (GPI-peptides). Fig. 6(A) shows the peptide/glycopeptide map obtained by LC/ITMS of Asp-N digested Thy-1. We localize the GPI-peptides using marker ions, EtN-PO_4-Man$^+$ at *m/z* 286 and GlcN-inositol-PO_4^+ at *m/z* 422, originating from the core structure of the GPI moiety by in-source CID (EtN, ethanolamine; GlcN, glucosamine). Mass chromatograms of *m/z* 286 and 422 suggest the locations of the GPI-peptides to be around 4.2 (peak A1-1) and 4.4 min (peak A1-2) (Fig. 6(B and C)). Using product ions originated from GPI moiety, such as GlcN-inositol-PO_4^+ and PO_4-Man-GlcN$^+$ (*m/z* 422 and 404), as marker ions, four product ion spectra of GPI-peptides were sorted out from all product ion spectra around peaks A1-1 and 1-2. Their precursor ions were doubly charged ions at *m/z* 1132 and 1213 (peak A1-1), 1051 and 1151 (peak A1-2). Based on these product ion spectra, we characterized GPI-peptides as the peptide Asp106-Cys111 with a GPI core structure plus Hex_{0-2}, $HexNAc_{1-2}$ and PO_4-EtN.

Fig. 7(A) shows the product ion spectrum of the doubly charged GPI-peptide ion at *m/z* 1051 in peak A1-2. In addition to product ions at *m/z* 422, those originating from the GPI moiety were detected at *m/z* 404 (PO_4-Man-GlcN$^+$), 447 (EtN-PO_4-Man-GlcN$^+$), 650 (EtN-PO_4-(HexNAc-)Man-GlcN$^+$), 787 (peptide-EtN$^+$), 868 (peptide-EtN-PO_4^+), 1191 (peptide-EtN-PO_4-Man-Man$^+$), 1477 (peptide-EtN-PO_4-Man-Man-(EtN-PO_4-)Man$^+$), 1638 (peptide-EtN-PO_4-Man-Man-(EtN-PO_4-)Man-GlcN$^+$), and 1898 (peptide-EtN-PO_4-Man-Man-(EtN-PO_4-)Man-GlcN-inositol-PO_4^+). From these fragments, it can be deduced that this peptide is Asp106-Cys111 carrying the GPI, as indicated in the inset in Fig. 7(A).

The other GPI-peptide in peak A1-1 was characterized as having side chains; -Hex attached to M1, -PO_4-EtN and -HexNAc attached to M3, based on the product ion spectrum of the doubly charged precursor ion at *m/z* 1132 (data not shown). These two GPI structures are identical to those that have been previously reported [24].

Product ion spectra of doubly charged ion at *m/z* 1151 and 1213 suggested that they contained GPI which bear one HexNAc or two Hex in addition to GPI in Fig. 7(A) respectively. Fig. 7(B) shows the product ion spectra of the doubly charged precursor ions at *m/z* 1151 in peak A1-2. In addition to *m/z* 422, we detected product ions at *m/z* 366 (HexNAc-Man$^+$), 447 (EtN-PO_4-Man-GlcN$^+$), 650 (EtN-PO_4-(HexNAc-)Man-GlcN$^+$), 1229 (peptide-EtN-PO_4-(HexNAc-)Man$^+$), 1391 (peptide-EtN-PO_4-(HexNAc-)Man-Man$^+$), 1676 (peptide-EtN-PO_4-(HexNAc-)Man-Man-(EtN-PO_4-)Man$^+$), 1838 (peptide-EtN-PO_4-(HexNAc-)Man-Man-(EtN-PO_4-)Man-GlcN$^+$), and 1880 (peptide-EtN-PO_4-(HexNAc-)Man-Man-(EtN-PO_4-)(HexNAc-)Man$^+$). These fragment ions suggest the attachment of -HexNAc to Man1, and -PO_4-EtN and -HexNAc to Man3 as indicated in the inset of Fig. 7(B). Similarly, product ion spectra of the doubly charged precursor ion at *m/z* 1213 indicate the attachment of 2Hex and HexNAc to Man1 and Man3-PO_4-EtN (data not shown). To our knowledge, this is the first report of these two GPI structures in Thy-1.

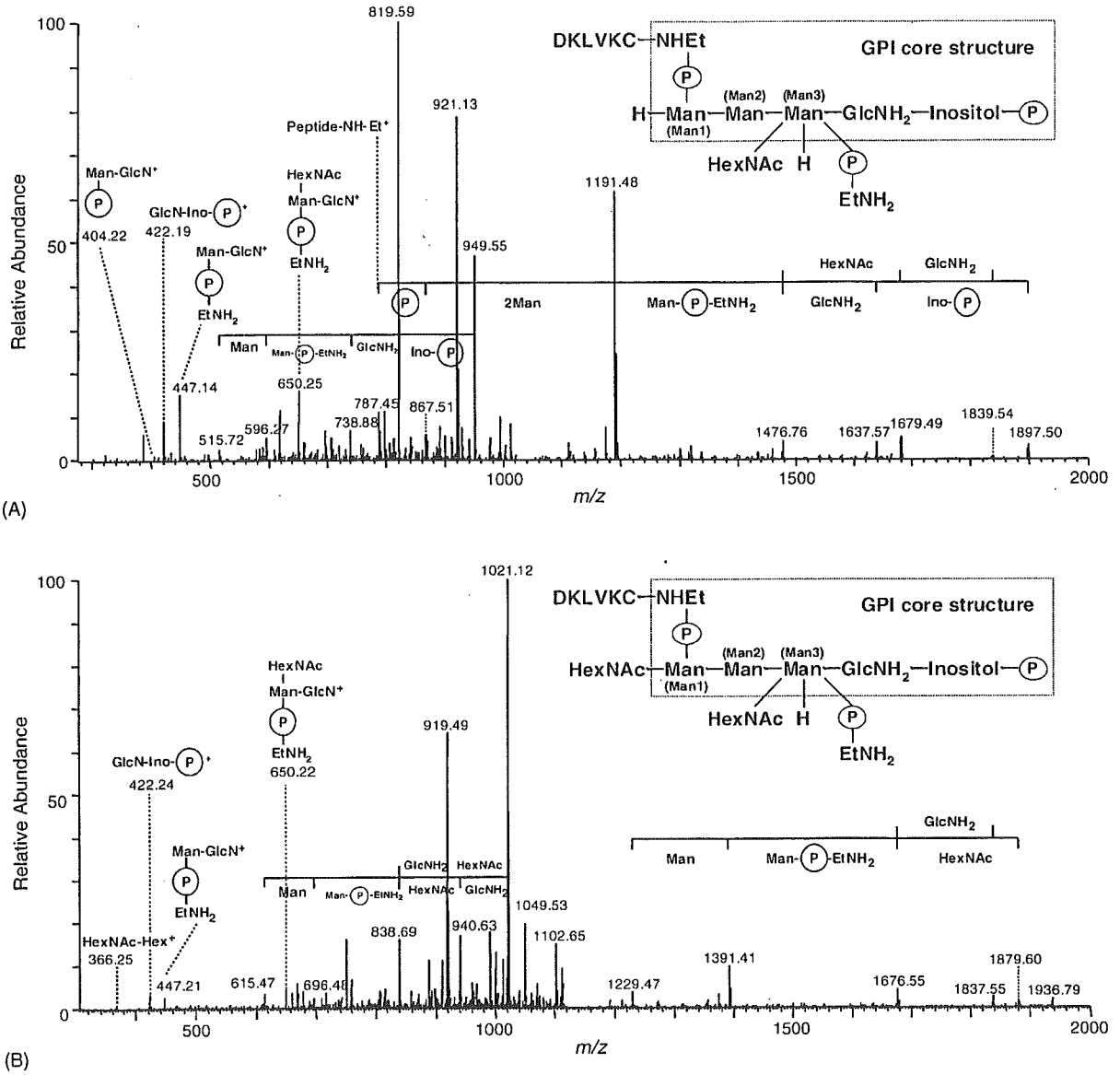

Fig. 7. Product ion spectra of the doubly charged GPI-peptide at *m/z* 1051 (A), and at *m/z* 1151 (B) in peak A1-2. The inset is the deduced structure of the GPI-peptide, and the core structure of GPI is the inside dashed line. Man, mannose; HexNAc, *N*-acetylhexosamine; $GlcNH_2$, glucosamine; $EtNH_2$-P, phosphorylethanolamine; Ino-P, inositol-phosphate.

3.5. Analysis of Asp-N digested Thy-1

Glycopeptides obtained by Asp-N digestion were also localized by in-source CID using marker ions at *m/z* 204 and 292 (Fig. 6(D and E)), and neutral loss of 81 u by data-dependent CID-MS/MS (Fig. 6(F)). Product ion spectra of glycopeptides were sorted by using B series ions as marker ions from those acquired around localized elution positions. Consequently, peaks A2-7 were identified as those of glycopeptides (Fig. 6(A)). The oligosaccharide structures in the glycopeptides were then characterized based on their product ion spectra (Table 1). In addition to the high-mannose-type oligosaccharides, M5, 6, and 7 deduced by LC/MS^n of tryptic digests, the oligosaccharide at Asn23 was characterized as $dHex_{0-1}Hex_{3,5,6}HexNAc_{3-5}NeuAc_{0,1}$, complex-type and hybrid-type oligosaccharides containing Lewis a/x or bisecting GlcNAc as a partial structure. Asn74 is attached by *N*-glycans with $dHex_{0-2}Hex_{3-6}HexNAc_{2,4,5}NeuAc_{0,1}$. They were high-mannose-type oligosaccharide, M5, complex-type oligosaccharides containing core Fuc and Lewis a/x as a partial structure, and hybrid-type oligosaccharides with core Fuc. Asn98 is occupied by high-mannose-type oligosaccharides, M5, and *N*-glycans with $dHex_{0-2}Hex_{3,5,6}HexNAc_{2-5}NeuAc_{0,1}$, hybrid-type oligosaccharides containing Lewis a/x or blood group H-determinant as a partial structure, which were found to be of greater diversity than those deduced by analysis of tryptic digests.

4. Discussion

In the present study, we have developed an efficient and convenient strategy for characterization, including protein identification and glycosylation analysis, of a small amount of unknown protein. We used gel electrophoresis, which is a powerful tool for separation of a small amount of protein from complex proteins mixture, especially from insoluble membrane fractions. For the complete glycosylation analysis, we examined the extraction of a whole glycoprotein from the gel, followed by trypsin digestion. Additionally, for the effective glycopeptide analysis, we studied mass spectrometric peptide/glycopeptide mapping by LC/MS^n with in-source CID and data-dependent MS^n. The glycopeptides were localized in the peptide/glycopeptide map by using oxonium ions as marker ions such as $HexNAc^+$ and $NeuAc^+$, which were generated by in-source CID, and neutral loss by data-dependent CID-MS/MS. For simultaneous identification of both peptides and glycopeptides, we conducted the database search analysis using search parameters containing a possible glycosylation at Asn with GlcNAc (203 Da). We successfully determined the sequences of peptides and some of the glycopeptides, which were localized by in-source CID and data-dependent CID-MS^n. The database search analysis using these search parameters was useful for identifying the glycopeptides resulting from predictable proteinase digestion. Glycopeptides caused by irregular digestion could be identified by assignment of peptide b and y series ions, which arose from further MS^n. The oligosaccharide structures of the identified glycopeptides were characterized on the basis of their product ion spectra. In this way, we were able to isolate rat brain Thy-1 and to elucidate *N*-glycosylation at Asn23, 74, and 98 as well as the structure of the GPIs at Cys111.

Post-translationally modified peptides could not be identified by the database search analysis. It has been particularly difficult to identify glycopeptides by database search analysis due to their complicated product ions resulting from the cleavage of glycosidic bonds. It has recently been reported that peptide + GlcNAc ion generated from a glycopeptide by CID-MS/MS yields b and y series ions by further MS^n, and that these ions can be utilized for identification of the peptide backbone and its glycosylation site [15,16,18]. Additionally, search analysis using the database including the possibility of glycosylation at Asn with all possible cleavage products of the known glycopeptides can be utilized for identification of glycopeptides in the peptide/glycopeptide map [19]. This ability would be helpful in the identification of glycoproteins whose glycosylation are already known. In the present study, we carried out a database search analysis using search parameters containing a possible glycosylation at Asn with only GlcNAc (203 Da), and successfully identified an unknown glycoprotein and *N*-glycosylated sites. This search analysis can be used for the identification of *O*-glycosylation, which has no consensus amino acid sequence, by using search parameters containing possible glycosylations at Ser/Thr with Hex, HexNAc, and dHex.

Precursor ion scans have been used for the localization the glycopeptides in peptide/glycopeptide mapping [10,11,13]. Although this method can be used for monitoring the peptides with predictable modification by setting mass of fragment ions prior to scanning, peptides with unpredictable modification cannot be detected. In contrast, in-source CID and CID-MS/MS are capable of localizing of the modified peptides after just one data acquisition using objective oxonium ions and neutral losses. In the present study, we were able to localize GPI-peptides in the peptide/glycopeptide map using $EtN\text{-}PO_4\text{-}Man^+$ and $GlcN\text{-}Inositol\text{-}PO_4^+$ generated by in-source CID [25] and to elucidate the GPI structures. We also could localize the glycopeptides with dHex, HexNAc, and NeuAc at the non-reducing ends as well as Hex using neutral loss by CID-MS/MS.

Site-specific glycosylation analysis of rat brain Thy-1 was performed after purification with monoclonal antibody affinity chromatography. Released oligosaccharides from fractionated trypsin-digested glycopeptides were analyzed by conventional analytical methods, including exoglycosidase digestion and methylation analysis [26]. In the present study, we separated PIPLC-treated GPI-anchored proteins of rat brain by SDS-PAGE, and conducted site-specific glycosylation analysis by LC/MS^n. Using a simpler step, we could elucidate the glycosylation at each glycosylation site with a greater variety of oligosaccharides than that reported previously and four GPI structures, including two novel attached structures.

Our strategy presented herein can relatively simply facilitate complete site-specific glycosylation analysis that used to require a series of complicated steps and is applicable to characterization of unknown proteins on 2-DE gel in proteomic study. Even in a mixture of multiple unknown glycoproteins, glycosylation of each glycoprotein can be determined based on the product ion spectra. Our method would be helpful for study of the alternation of glycosylation with growth, aging, and disease [27,28].

Acknowledgements

This study was supported in part by a Grant-in-Aid from the Ministry of Health, Labor and Welfare, Core Research for the Evolutional Science and Technology Program (CREST) of the Japan Science and Technology Agency (JST), and Research on Health Science focusing on Drug Innovation from The Japan Health Science Foundation (N.K.).

We appreciate Dr. A. Hachisuka of the National Institute of Health Science for her technical advice.

We would also like to thank Dr. M. Kubota and Mr. M. Yoshida of Thermo Electron K.K. (Japan), for their technical support.

References

[1] A. Varki, Glycobiology 3 (1993) 97.
[2] H. Sasaki, B. Bothner, A. Dell, M. Fukuda, J. Biol. Chem. 262 (1987) 12059.
[3] F. Wang, A. Nakouzi, R.H. Angeletti, A. Casadevall, Anal. Biochem. 314 (2003) 266.
[4] K. Hirayama, R. Yuji, N. Yamada, K. Kato, Y. Arata, I. Shimada, Anal. Chem. 70 (1998) 2718.
[5] M. Ohta, N. Kawasaki, S. Itoh, T. Hayakawa, Biologicals 30 (2002) 235.
[6] E. Mortz, T. Sareneva, S. Haebel, I. Julkunen, P. Roepstorff, Electrophoresis 17 (1996) 925.
[7] F.G. Hanisch, M. Jovanovic, J. Peter-Katalinic, Anal. Biochem. 290 (2001) 47.
[8] D. von Witzendorff, M. Ekhlasi-Hundrieser, Z. Dostalova, M. Resch, D. Rath, H.W. Michelmann, E. Topfer-Petersen, Glycobiology 15 (2005) 475.
[9] B. Küster, T.N. Krogh, E. Mortz, D.J. Harvey, Proteomics 1 (2001) 350.
[10] S.A. Carr, M.J. Huddleston, M.F. Bean, Protein Sci. 2 (1993) 183.
[11] M.J. Huddleston, M.F. Bean, S.A. Carr, Anal. Chem. 65 (1993) 877.
[12] R.S. Annan, S.A. Carr, J. Protein Chem. 16 (1997) 391.
[13] K. Sandra, I. Stals, P. Sandra, M. Claeyssens, J. Van Beeumen, B. Devreese, J. Chromatogr. A 1058 (2004) 263.
[14] A. Harazono, N. Kawasaki, T. Kawanishi, T. Hayakawa, Glycobiology 15 (2005) 447.
[15] U.M. Demelbauer, M. Zehl, A. Plematl, G. Allmaier, A. Rizzi, Rapid Commun. Mass Spectrom. 18 (2004) 1575.
[16] Y. Wada, M. Tajiri, S. Yoshida, Anal. Chem. 76 (2004) 6560.
[17] B. Sullivan, T.A. Addona, S.A. Carr, Anal. Chem. 76 (2004) 3112.
[18] S. Zhang, D. Chelius, J. Biomol. Tech. 15 (2004) 120.
[19] S. Wu, P. Bondarenko, T. Shaler, P. Shieh, W. Hancock, Thermo Finnigan LC/MS" Application Report Application Report No. 300.
[20] C. Bordier, J. Biol. Chem. 256 (1981) 1604.
[21] M.P. Lisanti, M. Sargiacomo, L. Graeve, A.R. Saltiel, E. Rodriguez-Boulan, Proc. Natl. Acad. Sci. U.S.A. 85 (1988) 9557.
[22] S. Itoh, N. Kawasaki, M. Ohta, T. Hayakawa, J. Chromatogr. A 978 (2002) 141.
[23] B. Domon, C.E. Costello, J. Glycoconjugate 5 (1988) 397.
[24] S.W. Homans, M.A. Ferguson, R.A. Dwek, T.W. Rademacher, R. Anand, A.F. Williams, Nature 333 (1988) 269.
[25] K. Fukushima, Y. Ikehara, M. Kanai, N. Kochibe, M. Kuroki, K. Yamashita, J. Biol. Chem. 278 (2003) 36296.
[26] R.B. Parekh, A.G. Tse, R.A. Dwek, A.F. Williams, T.W. Rademacher, EMBO J. 6 (1987) 1233.
[27] Y. Sato, M. Kimura, C. Yasuda, Y. Nakano, M. Tomita, A. Kobata, T. Endo, Glycobiology 9 (1999) 655.
[28] G. Durand, N. Seta, Clin. Chem. 46 (2000) 795.

A REPRINT FROM

ISSN 0915-7352
CODEN : TGGLEE

TRENDS IN GLYCOSCIENCE AND GLYCOTECHNOLOGY

GUIDE TO AUTHORS

TIGG is an international, bilingual journal of, by, and for the FCCA members, covering glycoscience and glycotechnology and issued bimonthly.

A. **MINIREVIEWS** describe recent progress in the fields of glycoscience and glycotechnology. Most are provided by request, but suggestions are always welcome in the form of a one-page synopsis (double spaced) addressed to the editor-in-chief.
B. **GLYCOTOPICS** are short commentaries on the latest papers describing outstanding findings with background.
C. **HOT PATENTS** describe recently released, exciting patents.
D. **GLYCOFORUM** is for our readers who wish to submit comments on scientific or social matters related to glycoscience and glycotechnology.
E. **LETTERS TO TIGG** are for readers who wish to discuss contributions appearing in TIGG or matters related to FCCA.

Readers are encouraged to contribute to any of the above. Manuscripts should be written in English and sent to the editor-in-chief. Due to limited space, not all manuscripts submitted for publication can be accepted. The editors hold the right to accept or reject and edit the manuscripts. All manuscripts accepted from non-Japanese contributors are translated into Japanese by our editorial staffs. The author contributing to the TIGG will be sent 30 reprint copies.

EDITOR-IN-CHIEF/TIGG International Editorial Office:
Ken-ichi KASAI, Department of Biological Chemistry, Faculty of Pharmaceutical Sciences,
Teikyo University, Sagamiko, Kanagawa 199-0195, JAPAN

Phone:81-426-85-3740, Telefax:81-426-85-3742, E-mail:kasai-k@pharm.teikyo-u.ac.jp

Membership yearly fee: for regular members ¥7,000; for student members ¥5,000; for supporting members (personal and enterprises), ¥52,000; for institutional members (libraries), ¥22,000. Issues are sent airmail, world-wide.

Correspondence should be addressed to FCCA Head Office/TIGG Domestic Editorial Office:
c/o Gakushin Publishing Co. Ltd., 1-1-8 Tarumi-cho, Suita 564-0062, Osaka, JAPAN
Phone: 81-6-6330-0956, Telefax: 81-6-6330-2724, E-mail: fcca@gak.co.jp

MINIREVIEW

Trends in Glycoscience and Glycotechnology
Vol.17 No.97 (September 2005) pp.193–203

Mass Spectrometry of Glycoproteins

糖タンパク質の質量分析

Kawasaki, Nana[*1,2]; Itoh, Satsuki[1]; Harazono, Akira[1]; Hashii, Noritaka[1,2]; Matsuishi, Yukari[1,2] Hayakawa, Takao[3]; and Kawanishi, Toru[1]

[1]Division of Biological Chemistry and Biologicals, National Institute of Health Science, 1-18-1, Kamiyoga, Setagaya-ku, Tokyo, 158-8501, Japan

[2] Core Research for Evolutional Science and Technology (CREST) of Japan Science and Technology Agency (JST), Kawaguchi Center Building, 4-1-8, Hon-cho, Kawaguchi, Saitama 332-0012, Japan

[3] Pharmaceutical and Medical Devices Agency, 3-3-2 Kasumigaseki, Chiyoda-ku, Tokyo, 100-0013, Japan

[*]Correspondence to: Nana Kawasaki, National Institute of Health Sciences, Division of Biological Chemistry and Biologicals, 1-18-1 Kamiyoga, Setagaya-ku, Tokyo, 158-8501, Japan

FAX: 81-3-3700-9084, E-mail: nana@nihs.go.jp

Key Words: *MS, MS/MS, MS^n, glycoprotein, oligosaccharide, glycopeptide*

Abstract

This review presents mass spectrometric methods for glycoprotein identification, determination of glycosylation sites, structural elucidation of carbohydrates, and their applications to glycomics and proteomics.

要　約

本レビューでは、質量分析を用いた糖タンパク質同定、糖鎖結合位置の決定、糖鎖構造解析、及びグライコミクス・プロテオミクスへの応用について紹介する。

A. Introduction

Mass spectrometry (MS) has become a powerful tool for glycoprotein identification, and the determination of glycosylation sites, and structural features of carbohydrates, such as sequence, linkage and branching at each glycosylation site. Generally, the mass spectrometric characterization of glycoprotein involves the following steps: 1) fractionation of enzymatically or chemically liberated glycans followed by MS, and 2) fractionation of glycopeptides from proteolytic digests followed by MS. Here we present the MS of glycan and glycopeptides using the latest applications.

B. MS of Liberated Glycans

Matrix-assisted laser desorption/ ionization (MALDI) (1), and electrospray ionization (ESI) (2), which are soft ionization techniques, are often used for glycan molecular mass determination. MALDI has been used by preference for rapid microanalyses, however, it generates metastable ions and the consequent various fragmentations, including the depletion of terminal sialic acids (known as post-source decay, PSD) (3). Although ESI used to have a problem with sensitivity, the introduction of nanospray technology allows us to use ESI to analyze femtomole levels of glycans (4). To measure all types of glycans, including neutral glycans and sulfated or sialylated acidic glycans, we suggest mass spectrometric glycan analysis in both positive and negative ion modes.

MALDI and ESI are combined with several types of

A. 緒　言

質量分析 (MS) は、糖タンパク質の同定、糖鎖結合位置の決定、並びに各結合位置における糖鎖の配列、結合位置、及び分岐等を含む構造特性解析の有用な手段として利用されている。現在、MS を用いた糖鎖解析のアプローチとしては、1) 酵素的または化学的に切り出された糖鎖の分画と MS、及び 2) 糖タンパク質酵素消化物からの糖ペプチドの分画と MS、が一般的である。そこで、ここでは、遊離糖鎖と糖ペプチドの MS について、最近の分析例を取り上げながら解説する。

B. 遊離糖鎖の MS

糖鎖分子の分析に適したソフトイオン化法として、マトリクス支援レーザー脱離イオン化法 (MALDI) (1)、及びエレクトロスプレーイオン化法 (ESI) (2) がよく利用されている. MALDI は迅速分析及び微量分析に適しているが、準安定イオンが生成し、MS^1 スペクトル上にはシアル酸が脱離したイオンをはじめとする様々なフラグメントが検出される (ポストソース分解、PSD) (3)。ESI は感度上の問題が指摘されてきたが、現在ではナノスプレーの開発によって、フェムトモルレベルの糖鎖分析が可能となっている (4)。糖鎖には中性糖鎖だけでなく、シアル酸や硫酸基などが結合した酸性糖鎖が存在するので、未知試料を分析する際には、ポジティブ及びネガティブ両イオンモードで測定するのが望ましい。

MALDI や ESI は様々なアナライザー (分析計) と組み合

analyzer, such as quadrupole (Q) (5), quadrupole ion trap (IT) (6), time-of-flight (TOF) (7), and Fourier transform ion cyclotron resonance (FTICR) (8). Tandem mass spectrometers with various combinations of these analyzers have recently become available. Tandem mass spectrometry (MS/MS) is widely recognized as an effective means of structural elucidation, including molecular mass measurement by MS^1 and oligosaccharide sequencing by collision-induced dissociation (CID)-MS/MS (9–11). In particular, ITMS instruments are becoming popular for multistage tandem mass spectrometry (MS^n), which offers multiple precursor selections and CID experiments (12, 13).

Fig. 1A shows types of carbohydrate fragmentation by CID-MS/MS (14). In the positive ion mode the most common fragmentation involves cleavage of the glycosidic bond with retention of the glycosidic oxygen atom by species formed from the reducing end (Fig. 1B). Fragment ions generated by this cleavage are represented as B-ion (non-reducing end) and Y-ion (reducing end). The cleavage of carbon-carbon bonds of the sugar ring yields A-ion and X-ion. These cross ring fragments are often used as decisive ions in linkage determination (15, 16).

Fig. 2 shows the positive ion ESI-MS/MS and MS^3 spectra of pyridylaminated agalacto-triantennary oligosaccharide (I) (Figs. 2A, A') and bisected agalacto-biantennary oligosaccharide (II) (Figs. 2B, B'). These are positional isomers whose one GlcNAc is attached to either α1-3/6 Man or β1-4Man in the trimannosyl core and cannot

わせて利用されている。アナライザーには四重極型 (Q) (5)、イオントラップ型 (IT) (6)、飛行時間型 (TOF) (7)、及びフーリエ変換イオンサイクロトロン共鳴型 (FTICR) (8) MS 装置などが用いられている．現在では、これらの分析装置を様々に組み合わせたタンデム質量分析装置の利用が可能である。タンデム質量分析 (MS/MS) は、MS^1 による糖鎖の質量測定と、衝突誘起解離 (CID)-MS/MS による糖鎖の配列解析を同時に行うことができる (9–11)。特に ITMS 装置は、前駆イオンの選択と CID-MS/MS を繰り返す多段階 MS/MS (MS^n) が可能であることから、近年、糖鎖解析用装置としての人気が高い (12、13)。

図 1A は、CID-MS/MS における糖鎖の開裂を示したものである (14)。ポジティブイオンモードで測定した糖鎖の CID-MS/MS では主に、グリコシド結合の酸素原子を還元末端側糖鎖に残した開裂が生じる (図 1B)．そのとき生じた非還元末端側イオンは B イオン、還元末端側イオンは Y イオンと呼ばれ、糖鎖の配列解析に利用される。ピラノース環の炭素 - 炭素間の結合が開裂して生じたイオンは A、及び X イオンと呼ばれ、糖鎖結合位置の決め手となることがある (15、16)。

図 2 は、ピリジルアミノ化されたアガラクト 3 本鎖糖鎖 (I) 及びアガラクトバイセクト 2 本鎖糖鎖 (II) のポジティブイオン MS/MS (図 2A、B)、及び MS^3 (図 2A'、B') スペクトルである。これらの糖鎖は GlcNAc 1 分子がトリマンノシルコアの α1-3/6Man または β1-4Man に結合した位置異性体で、MS^1 による分子量測定では区別することはできない。しかし、MS^n によっ

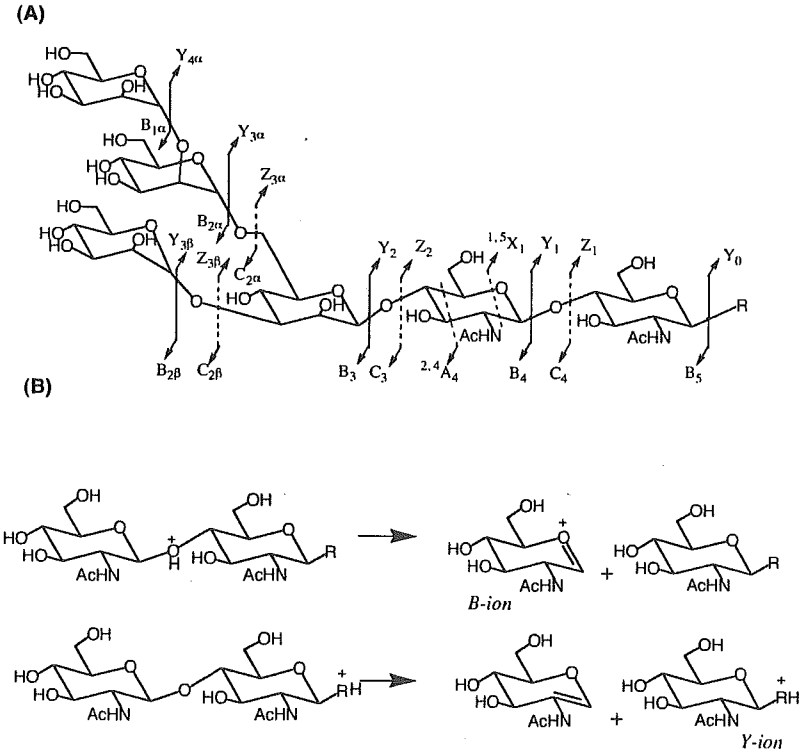

Fig. 1. (A) Types of carbohydrate fragmentation. (B) Production of B- and Y-ions in the positive ion mode.

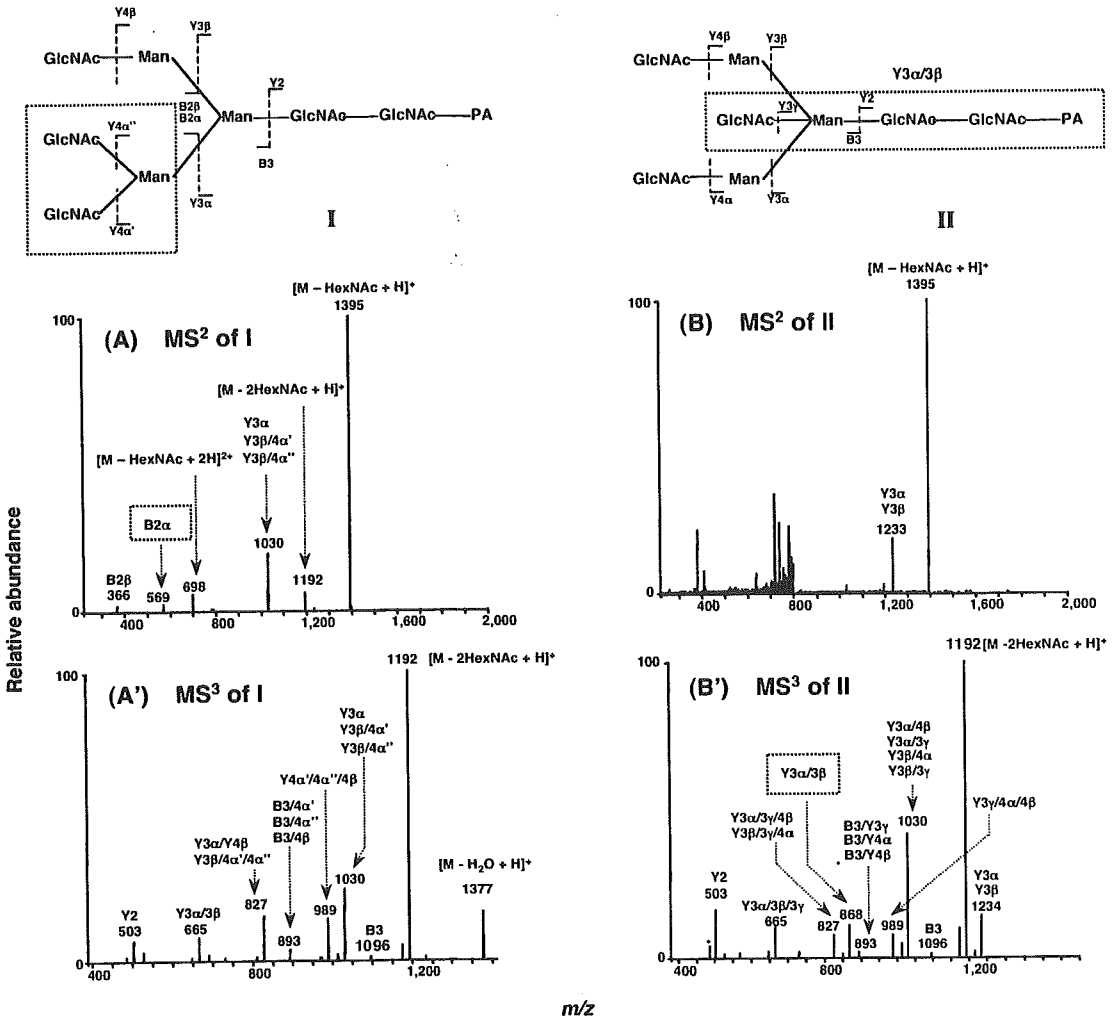

Fig. 2. MS^n spectra of oligosaccharides. (A) MS/MS spectrum of oligosaccharide I (precursor ion: *m/z* 800.8). (A') MS^3 spectrum of oligosaccharide I (precursor ion: *m/z* 1,395.4). (B) MS/MS spectrum of oligosaccharide II (precursor ion: *m/z* 800.5). (B') MS^3 spectrum of oligosaccharide II (precursor ion: *m/z* 1,395.4). MS: LTQ (Thermo Electron).

be discriminated by MS^1 (molecular mass determination). In contrast, MS^n spectra clearly show structural differences between two glycans. B-ion corresponding to $GlcNAc_2Man^+$ is observed at *m/z* 569 in the MS/MS spectrum of glycan I (Fig. 2A), while Y-ion at *m/z* 868 corresponding to [GlcNAc-Man-GlcNAc-GlcNAc-PA + H]$^+$ is detected in MS^3 spectrum of glycan II (Fig. 2B'). In particular, glycan II can be determined as bisected oligosaccharides on the basis of a bisected *N*-glycan diagnostic ion at *m/z* 868.

The MS^n spectra of some glycans exhibit characteristic fragment patterns. Hence, even if no diagnostic ion, such as a bisected glycan-specific fragment, is detected, the glycan structure can be sometimes deduced from ion intensity ratios obtained by MS^n (17,18). For instance, structures of branched arms were deduced from mass spectrometric patterns obtained by MS/MS which causes a cleavage of α1-3 linkage more than α1-6 linkage (19–21). However, complete structural

て両者の構造の違いを明確にすることができる。例えば、糖鎖 I の MS/MS スペクトルには *m/z* 569 に $GlcNAc_2Man^+$ に相当する B イオンが検出され（図 2A）、糖鎖 II の MS^3 スペクトル（前駆イオン：*m/z* 1395 [M-HexNAc + H]$^+$）には [GlcNAc-Man-GlcNAc-GlcNAc-PA + H]$^+$ に相当するイオンが *m/z* 868 に検出されている（図 2B'）。特に、[GlcNAc-Man-GlcNAc-GlcNAc-PA + H]$^+$ (*m/z* 868) はバイセクト糖鎖に特異的なフラグメントであり、糖鎖 II がバイセクト糖鎖であることを決定づけている。

糖鎖の MS^n は特徴的なスペクトルパターンを示すことが多いので、構造特異的イオンが検出されない場合でも、MS^n スペクトルのパターンより糖鎖構造を推定できる場合がある (17、18)。例えば、トリマンノシルコアの α1-3 結合が α1-6 結合よりも開裂しやすいことを利用して、分岐構造を解析した例が報告されている (19–21)。しかし、MS 単独で糖鎖構造を完

elucidation by MS alone is still a great challenge, and additional experiments are required, such as exoglycosidase digestion (22), lectin affinity chromatography (23), and sugar mapping (17,24,25).

C. Glycan Profiling by LC/MS

Many different oligosaccharides are attached to a glycoprotein. The development of derivatization and separation techniques for glycans has been an important part of structural glycobiology (26–34). The derivatization of glycan with a hydrophobic molecule improves the ionization efficiency of hydrophilic glycans and offers higher sensitivity (31,35). A combination of various HPLC techniques with off-line MALDI-MS or on-line ESI-MS has been successful in oligosaccharide profiling as well as the elucidation of structural details (36–39). As an example, we present the mass spectrometric *N*-glycan profiling of CHO cells and cells transfected with *N*-acetylglucosaminyltransferase III, which catalyzes the addition of GlcNAc to β1-4Man in the trimannosyl core (Fig. 3) (40). Mass spectrometric analysis reveals the difference in glycosylation between two samples and the appearance of peaks with additional HexNAc (203 Da) in the transfected cells.

We recently demonstrated quantitative oligosaccharide

全に同定することが困難である場合が多く、MSはエキソグリコシダーゼによる段階的消化法(22)、レクチンアフィニティークロマトグラフィー(23)、及び糖鎖マッピング(17、24、25)などと組み合わせて用いられることが多い。

C. LC/MSを用いた糖鎖プロファイリング

糖タンパク質には様々な糖鎖が結合しているので、糖鎖の標識法と分離技術の開発は、構造糖鎖生物学において重要な位置を占めている(26–34)。糖鎖を分離・検出するために開発された疎水性物質による誘導体化は、親水性の高い糖鎖のイオン化効率を向上させるので、MSにおける高感度化においても有用である(31、35)。さらに、様々なHPLCによる分離法とオフラインMALDI-MS、あるいはオンラインESI-MSを組み合わせた分析方法は、糖鎖プロファイリングと糖鎖構造解析を兼ね備えた方法として利用され、多くの成果を上げている(36–39)。一例として図3にCHO細胞、及びトリマンノシルコアのβ1-4ManにGlcNAcを付加させる*N*-アセチルグルコサミン転移酵素III(GnT-III)遺伝子を導入したCHO細胞のMSを用いた糖鎖プロファイリングの結果を示す(40)。MSを利用することによって、GnT-III導入細胞で新たに出現した糖鎖は、HexNAc1分子(203Da)増加した糖鎖であることが確認できる。

筆者らは最近、安定同位体標識化2-アミノピリジン(AP)を用いた標識法とLC/MSを組み合わせた定量的糖鎖プロファ

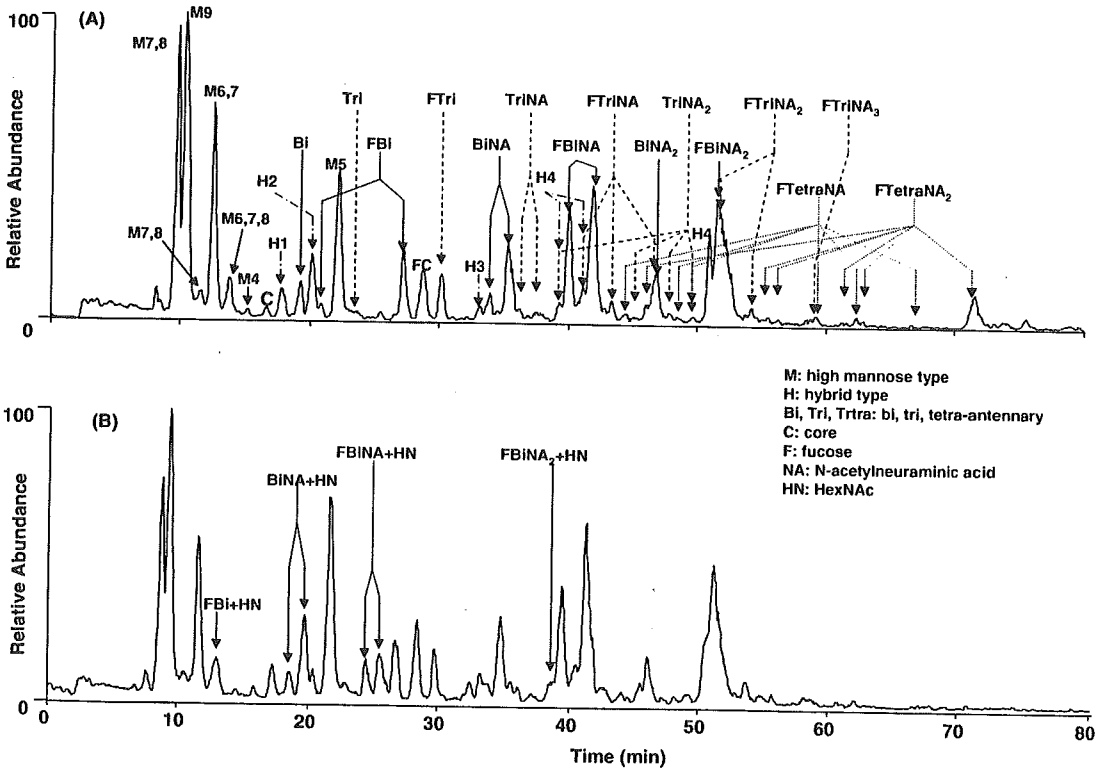

Fig. 3. TICs of *N*-linked oligosaccharides released from the insoluble fractions. (A) CHO cells. (B) *N*-acetyl glucosaminyltransferase III-transfected CHO cells. Column: Hypercarb (0.2 × 150 mm, Thermo Electron), LC: Magic 2002 (Michrome BioResources), MS: TSQ-7000 (Thermo Electron), Eluent: 5 mM ammonium acetate containing acetonitrile.

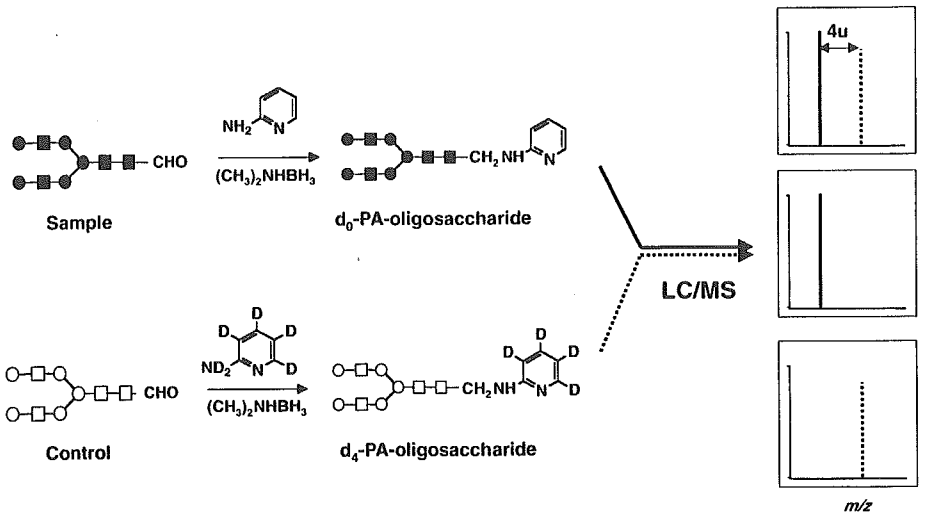

Fig. 4. Quantitative oligosaccharide profiling using LC/MS and an isotope tagging method.

profiling using isotope-labeled 2-aminopyridine (AP) and LC/MS (Fig. 4) (41). In this procedure, oligosaccharides released from an analyte and standard glycoprotein are tagged with d_0-AP and d_6-AP, respectively, and an equal amount of d_0-PA and d_4-PA oligosaccharides is analyzed by LC/MS. Oligosaccharides existing in either the analyte or standard glycoprotein appear as single ions, and oligosaccharides that exist in both analyte and standard glycoprotein are detected as paired ions with a difference of 4 u. The relative amount of analyte oligosaccharides can be determined on the basis of the analyte/ internal standard ion pair intensity ratio. This method can improve the precision of the mass spectrometric quantification and be used for glycan differential analysis among multiple samples.

D. MS of Glycopeptides

When glycans are released from protein, all information about their attachment to the protein is lost. Protein identification, determination of glycosylation sites and site-specific glycosylation analyses are generally achieved by the mass spectrometric analysis of glycopeptides. ESI and MALDI coupled with several analyzers are employed for glycopeptide analysis. ESI allows the accurate mass measurement of relatively large glycopeptide/protein because of the generation of multiple charged ions, whereas ions of large glycopeptide molecule ions are sometimes missed by MALDI-MS due to PSD and their poor ionization efficiency (42).

Fig. 5 illustrates three possible cleavages of the peptide backbone. The most common C-terminal and N-terminal fragment ions are b-ion and y-ion, respectively (37). In many cases, CID induces glycosidic bond cleavages rather than peptide backbones. Electron capture dissociation with FT-ICRMS is reported as a means for preferential cleavage of the

イリングを開発した(図4)(41)。この方法は、標準糖タンパク質及び検体糖タンパク質から切り出した糖鎖をそれぞれ6重水素置換AP(d_6-AP)、及び未置換AP (d_0-AP)で標識し、得られたd_4-PA糖鎖及びd_0-PA糖鎖を1対1の混合物としてLC/MSで分析するものである。標準糖タンパク質または検体糖タンパク質のどちらか一方にしか結合していない糖鎖は、d_4-PA糖鎖またはd_0-PA糖鎖どちらかの単独イオンとして検出される。標準糖タンパク質及び検体糖タンパク質に共通して存在する糖鎖は4u異なる1対のイオンとして検出され、d_4-PA糖鎖及びd_0-PA糖鎖のイオン強度比から相対糖鎖結合量を求めることができる。同位体標識糖鎖を内部標準物質として用いることによって、MSを用いた定量解析における再現性が改良されるので、定量的糖鎖プロファイリングは、複数のサンプル間の糖鎖の差異を質的量的に比較する場合に有用である。

D. 糖ペプチドのMS

タンパク質から糖鎖を切り離すと、糖鎖とタンパク質間の結合に関する情報が失われてしまうので、糖鎖含有タンパク質の同定、糖鎖結合位置の決定、及び部位特異的糖鎖不均一性の解析などには糖ペプチドのMSが適している。糖ペプチドの分析においても、ESIあるいはMALDIに様々なアナライザーを組み合わせた装置が利用されている。MALDI-MSでは、ほぼ一価イオンが生成するが、ESI-MSでは多価イオンが生成するため比較的高分子量の糖ペプチドの質量を正確に測定することが可能である。また、MALDI-MSを用いて糖鎖の割合が高い糖ペプチドを分析する場合、イオン化の抑制やPSDによって、分子関連イオンが測定されにくいとする報告がある(42)。

図5はペプチド骨格の開裂を示している。ペプチド結合の開裂によって生じたN末端側はbイオン、C末端側はyイオンと呼ばれる(43)。通常、糖ペプチドのCID-MS/MSでは、ペプチドよりも糖鎖の開裂が優先される。ペプチド部分が優先的に開裂する方法としてFT-ICRMS装置を用いた電子捕獲解

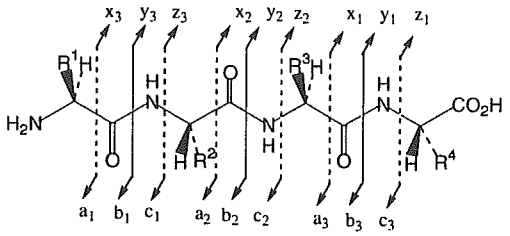

Fig. 5. Types of peptide fragmentation.

peptide backbone (44,45).

For the cleavages of both glycosidic and peptide bonds CID-MS/MS is carried out with relatively high energy (approx. 50V/1000 u) (46–51). Hence, it allows both peptide sequencing and estimation of the carbohydrate structure on the basis of b/y-ions and B/Y-ions. Fig. 6A presents the CID-MS/MS spectrum of a glycopeptide derived from human α-fetoprotein using the ESI-QqTOFMS instrument. Carbohydrate-specific B-ions, such as $HexNAc^+$ and $NeuAc^+$ are observed at *m/z* 204, 292 as well as y-series ions. Based on the y-series ions and peptide ion, this peptide is identified

離法が報告されている(44、45)。

糖鎖とペプチド部分を同時に開裂させるためには比較的高いエネルギー(約50V/1000 u)を与えてCID-MS/MSを行う(46–51)。生成したb、yイオン、及びB、Yイオンから、ペプチド部分のアミノ酸配列や、糖鎖構造を解析することができる。図6Aは、ESI-四重極飛行時間型MSを用いたCID-MS/MSによって得られたヒトアルファフェトプロテイン由来糖ペプチドのMS/MSスペクトルである。糖鎖Bイオンである*m/z* 204 ($HexNAc^+$)、及び292 ($NeuAc^+$)等と一緒に、ペプチドに由来する一連のyイオンが検出されていることがわかる。これら一

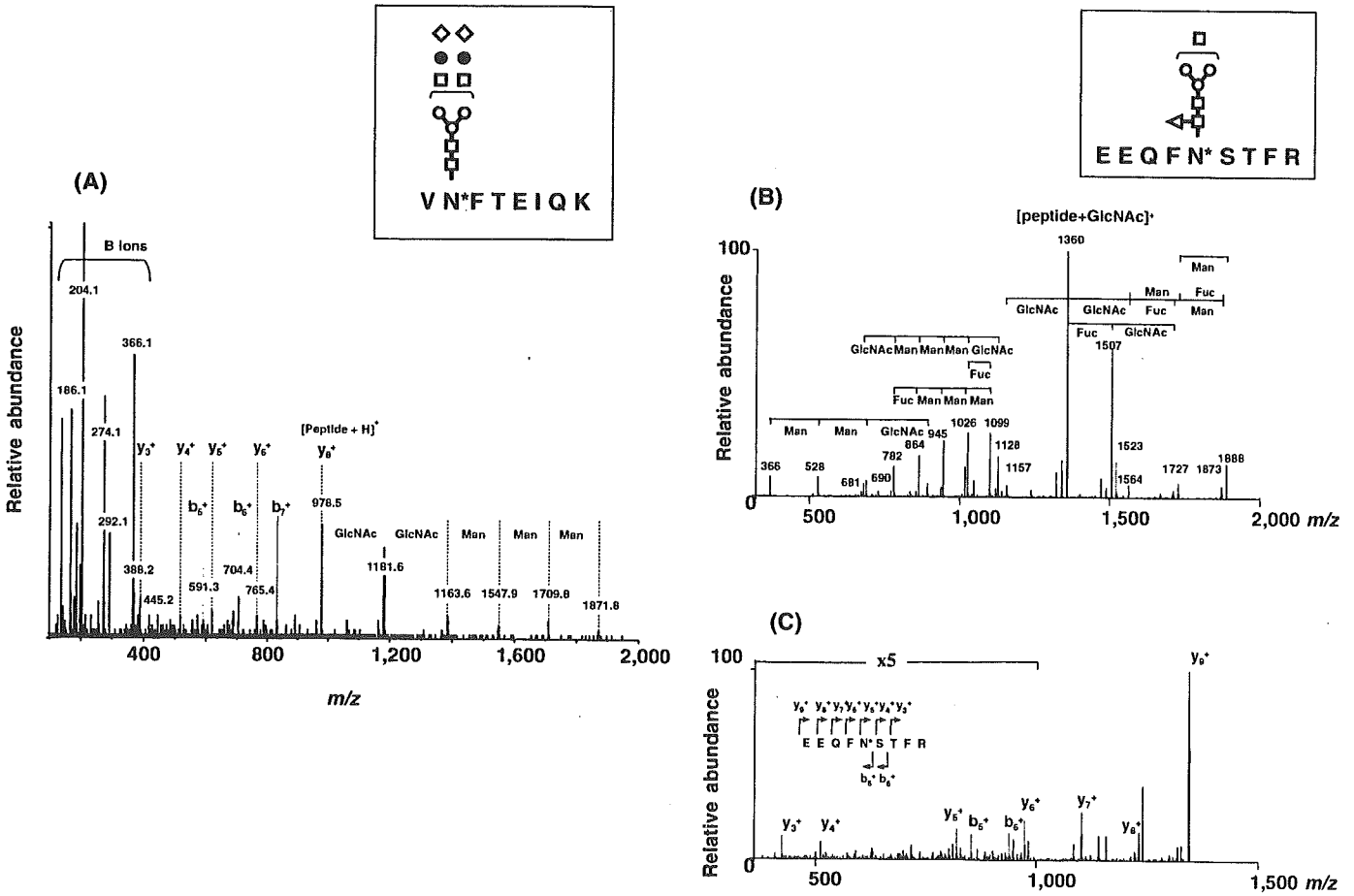

Fig. 6. CID-MS^n spectra of glycopeptides. (A) CID-MS/MS with relatively high energy (precursor ion, *m/z* 1,061.8), Sample: glycopeptide from human alpha-fetoprotein, MS: QSTAR (Applied Biosystems). (B) Low-energy CID-MS/MS (precursor ion, *m/z* 1,200). (C) Low-energy CID-MS^3 (precursor ion, *m/z* 1,360), Sample: glycopeptide from mouse IgG1, MS: LTQ (Thermo Electron).

as VNFTEIQK. The oligosaccharide structure can be deduced as disialylated biantennary from the molecular mass of the carbohydrate moiety together with B-ions in the MS/MS spectrum.

B- and Y-series ions are produced by the low-energy CID-MS/MS of glycopeptides (12, 52–55). Fig. 6B shows the low energy (approx. 5–20V/1000 u) CID-MS/MS spectrum of glycopeptide derived from mouse IgG1. Based on the carbohydrate related-ions, the carbohydrate structure could be determined as fucosylated biantennary. When using an ITMS instrument, MS^3 is automatically carried out for intense ions. In this experiment, [peptide +HexNAc +H]$^+$, which is generally detected as intense ion, was subjected to further product ion scan, and b- and y-series ions appeared in the MS^3 spectrum (Fig. 6C). Peptides can be identified by comparing experimental fragment ions with predictable fragment ions derived from proteins in a database. Moreover, the database analysis with the possibility of glycosylation at Asn and Ser/Thr with HexNAc, Hex, and dHex allows the identification of glycopeptides and glycosylation sites (56). For instance, this peptide was identified as EEQFN*STFR glycosylated with HexNAc at N*. This method would enable the glycosylation analysis of unknown glycoproteins and a mixture of glycoproteins.

E. Site-Specific Glycosylation Analysis of Glycoproteins

Fig. 7 illustrates the strategy for the site-specific glycosylation analysis of glycoproteins. First, a glycoprotein is digested with an appropriate proteinase, which provides

連のｙイオン、及びペプチドイオンの質量から、このペプチド部分はVNFTEIQKと同定することができる。また、糖鎖構造は、糖鎖部分の分子量とBイオンからジシアロ２本鎖糖鎖と推定される。

低エネルギーCID-MS/MSでは、グリコシド結合が優先して開裂し、B、及びＹイオンが検出される(12、52–55)。図6Bはマウス IgG1から得られた糖ペプチドの低エネルギーCID-MS/MS(約5-20V/1000 u)スペクトルで、糖鎖関連イオンから、糖鎖構造を推定することができる。糖ペプチドのMS/MSでは一般に、[ペプチド＋HexNAc＋H]$^+$が比較的強く検出される。そこで、ITMS装置を用いて[ペプチド+HexNAc＋H]$^+$を前駆イオンとして選択し、さらにプロダクトイオンスキャンを行うと、MS^3スペクトル上にｂ及びｙイオンが検出される(図6C)。これらのｂ及びｙイオンの実測値をタンパク質データベースに登録されているタンパク質の予測プロダクトイオンの理論質量と比較することによって、ペプチドを同定することができる．さらに、AsnやSer/ThrにHexNAc、Hex、あるいはdHex等による糖鎖修飾の可能性を追加してデータベース検索をすることによって、糖鎖結合位置を決定できる場合がある(56)。例えば、ここで分析された糖ペプチドはデータベース検索エンジンを用いて、EEQFN*STFR(N*はHexNAc修飾Asn)と同定された。この方法を利用することによって、混合物中の糖タンパク質や、未知の糖タンパク質の部位特異的な糖鎖解析が可能となるものと期待される。

E. 糖タンパク質の部位特異的糖鎖解析

糖タンパク質の部位特異的糖鎖解析の流れを図７にまと

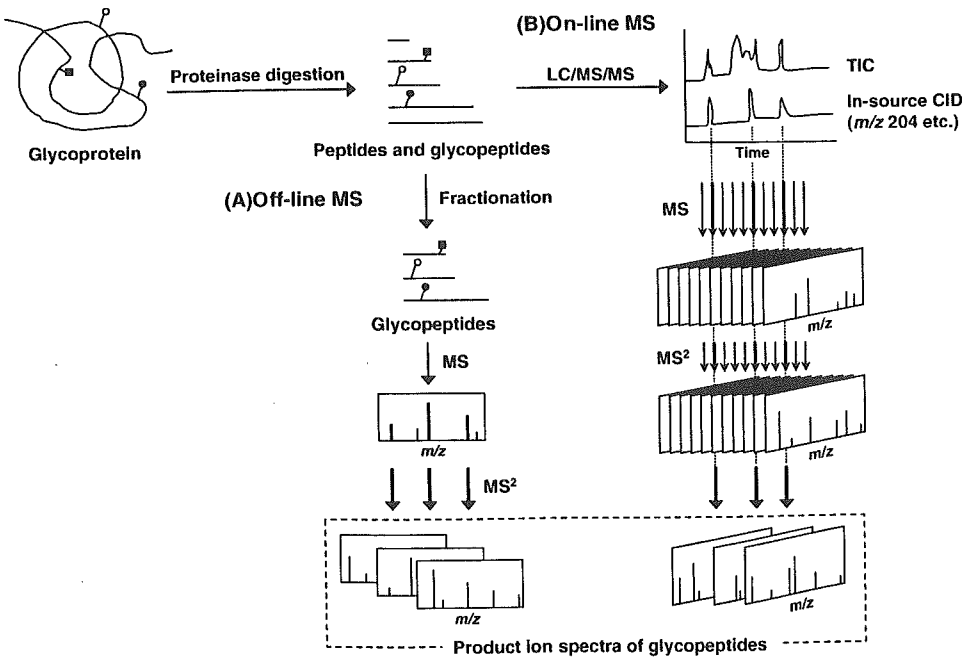

Fig. 7. Strategy for site-specific glycosylation analysis by LC off-line MS (A) and on-line LC/MS (B).

glycopeptides, including a single glycosylation site. Trypsin, Lys-C, Glu-C and Asp-N are commonly used for glycosylation analysis. Since glycopeptide ions are sometimes missed by MS in the presence of excess peptides due to their lower ionization efficiency, several methods have been proposed for the fractionation of glycopeptides, such as HPLC and affinity chromatography (57,58), followed by off-line MALDI-MS. LC on-line ESI/MS is an efficient method for the direct elucidation of glycopeptides in a complex mixture. Although LC/MS provide a complicated chromatogram, glycopeptides in a choromatographic position can be localized by the appearance of marker ions, such as $HexNAc^+$ and $HexHexNAc^+$, resulting from precursor ion scanning and in-source CID (59–66). However, for peptide identification these two means require additional CID-MS/MS scan for some intense ions (data-dependent CID-MS/MS scan). Recently we presented an alternative method, with which product ion spectra of glycopeptides can be selected directly using marker ions arising from glycopeptides by data-dependent CID-MS/MS scan with relatively high energy (49).

める。まず、糖タンパク質を適切な酵素で糖ペプチドに断片化する。この際、同一ペプチドに複数の糖鎖結合部位が含まれないように酵素を選択する。基質特異性の高いトリプシン、Lys-C、Glu-C、及びAsp-N等がよく用いられている。糖ペプチドはペプチドに比べてイオン化効率が悪く、ペプチドが混在するとマススペクトルが得られにくい。そのため、アフィニティークロマトグラフィーや、HPLC等で予め糖ペプチドを分画してから(57、58)、マススペクトルを測定するオフライン法(図7A)や、C18カラム等を用いたLC/MSでペプチド・糖ペプチドを分離しながら直接マススペクトルを測定するオンライン法がよく用いられている(図7B)。オンラインLC/MSでは複雑なクロマトグラムが得られるが、プリカーサーイオンスキャンやインソースCIDによって生じた糖鎖に特徴的なBイオン(例えば、$HexNAc^+$、m/z 204や$HexHexNAc^+$、m/z 366など)を利用することによって、糖ペプチドの溶出位置を推定することができる(59–66)。ただしこれらの方法は、ペプチドを同定するために、別途、強度の高いイオンに対する自動的CID-MS/MSスキャン(データ依存的CID-MS/MSスキャン)を行う必要がある。そこで、我々は別法として、データ依存的なCID-MS/MSによって生成したBイオンを利用して糖ペ

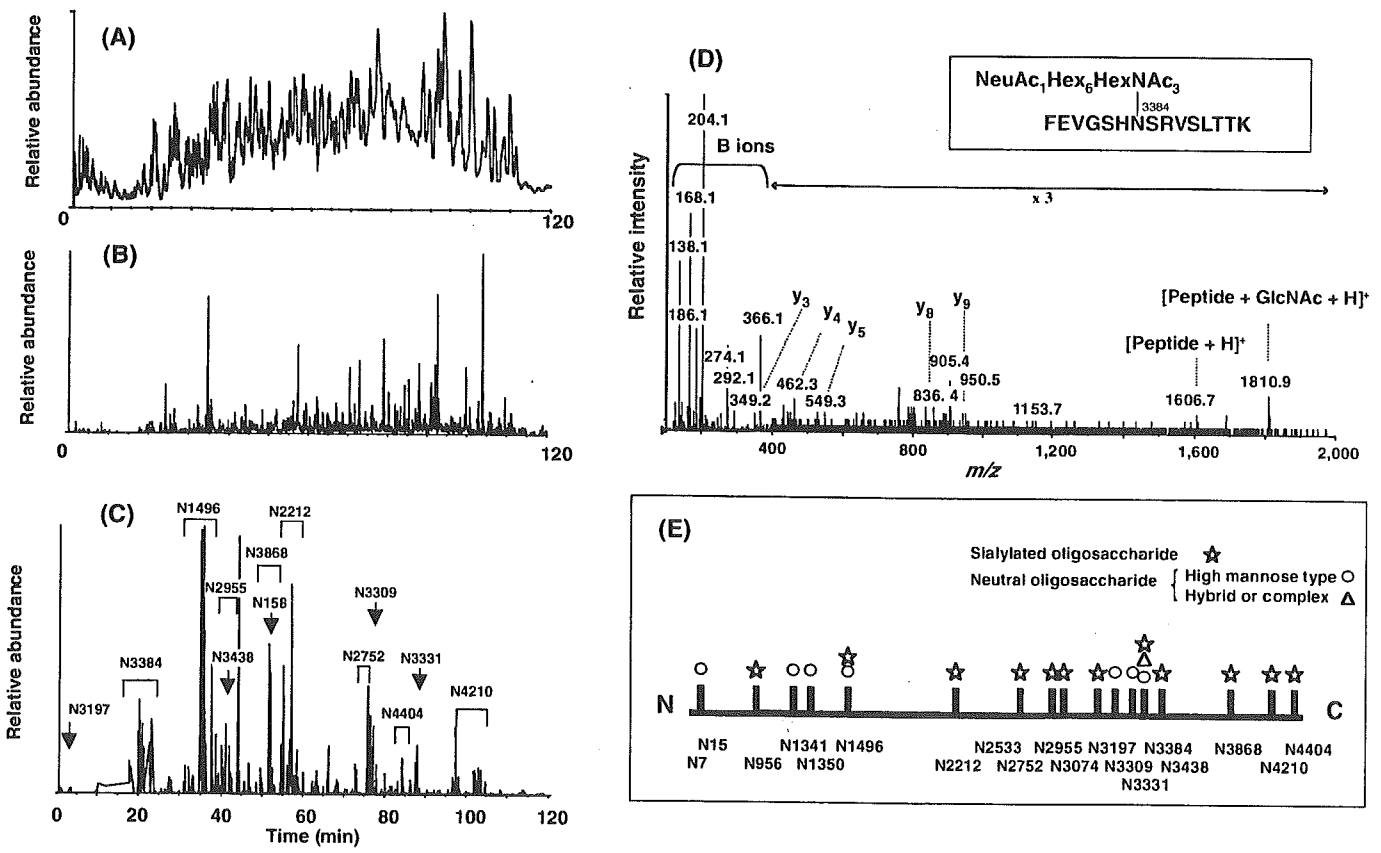

Fig. 8. Site-specific glycosylation analysis of apoB100 by LC/ESI-MS/MS. (A) TIC of full MS scan (m/z 400-2,000). (B) TIC of data-dependent CID-MS/MS scan (m/z 100-2,000). (C) Mass chromatogram at m/z 204 in data-dependent CID-MS/MS scan. (D) MS/MS spectrum of glycopeptide (precursor ion: m/z 1,160.4). (E) *N*-glycosylation of apoB100. Sample: tryptic digest of apoB100 (4 μg), LC: Paradigm (Michrome BioResources), Column: Magic C18 (0.2 × 50 mm, Michrome BioResources), MS: QSTAR (Applied Biosystems).

Here we demonstrate the site-specific glycosylation analysis of human apolipoprotein B100 (apoB100). Tryptic digest of apoB (4 μg) was injected into an LC/ESI-QqTOFMS instrument equipped with a C18 column. Figs. 8A and B are total ion chromatograms (TIC) obtained by full MS^1 scan and data-dependent CID-MS/MS scan, respectively (49). These chromatograms appear complicated due to a number of peptide-related ions derived from a large glycoprotein molecule of 500,000 Da. In order to localize glycopeptides in the peptide map, carbohydrate marker ion, $HexNAc^+$ at *m/z* 204, was extracted from the TIC of data-dependent CID-MS/MS scan (Fig. 8C). The MS/MS spectra of glycopeptides were then sorted from the peaks appearing in the mass chromatogram (Fig. 8D). We successfully identified 17 *N*-glycosylation sites among 19 potential *N*-glycosylation sites and deduced glycosylation at each glycosylation site from the mass of carbohydrate moieties (Fig. 8E).

F. Application in Proteomics and Glycomics

MS enables us to elucidate a small number of glycoproteins isolated by electrophoresis (67, 68) and micro HPLC (69). This method could be applied in comprehensive or carbohydrate structure-specific glycoprotein analysis by a combination with proteomic approaches such as 2-dimensional (2D) gel electrophoresis (GE) and 2D-LC followed by MS. Some applications have been already demonstrated, for instance, glycoprotein expression analysis using 2D-GE coupled with carbohydrate-specific dyeing or immunoblotting (70), and LC/MS combined with lectin affinity chromatography (71,72). These glycomic/proteomic technologies are expected to be a powerful tool for the functional study of glycoproteins, finding disease-related glycoproteins and identifying proteins attached to some glyco-epitopes.

プチドのMS/MSスペクトルを選び出す方法を見出した(49)。

図8に、我々が最近行ったオンライン法によるヒトアポリポプロテインB100 (apoB100)の部位特異的な糖鎖解析例を示す(49)。apoB100のトリプシン消化物(4 μg)をC18カラムを用いたLC/ESI-QqTOFMS装置で分析した。図8A及びBはフルMS^1スキャン(*m/z* 1,000-2,000)及びデータ依存的CID-MS/MSスキャンによって得られたトータルイオンクロマトグラム(TIC)である。apoB100は分子量約500,000 Daの大きな糖タンパク質なので、非常に多くのペプチドイオンが検出されている。そこで、糖ペプチドの溶出位置を推定するために、データ依存的CID-MS/MSスキャンによって生じた*m/z* 204イオンのみを抜き出した(図8C)。出現したピーク周辺からBイオンを指標に糖ペプチドのMS/MSスペクトルを探し出し、それらのスペクトル上のプロダクトイオンを帰属した(図8D)。その結果、19カ所の推定*N*結合型糖鎖結合部位のうち17カ所に糖鎖が結合していることを明らかにするとともに、それぞれの部位に結合している糖鎖を推定することができた(図8E)。

F. グライコミクス・プロテオミクスへの応用

現在では、電気泳動(67,68)やミクロ液体クロマトグラフィー(69)で分離された僅かな糖タンパク質からでも、MSによって、多くの糖鎖構造情報を得ることができるようになった。これらの糖鎖解析技術とプロテオミクス的アプローチ、すなわち、2次元電気泳動や2次元クロマトグラフィーによるタンパク質発現解析とMSを組み合わせることによって、糖タンパク質の網羅的解析や、任意の糖鎖構造を持つタンパク質の解析が可能になるものと期待されている。すでに、2次元電気泳動と糖タンパク質特異的染色法や免疫ブロットを組み合わせた糖タンパク質発現解析や(70)、レクチンアフィニティークロマトグラフィーと各種LC/MSを組み合わせた糖タンパク質の網羅的解析の例が報告されている(71,72)。今後、これらのグライコミクス・プロテオミクス解析技術が、糖鎖の機能研究や、疾患等に関与する糖鎖・糖タンパク質の探索、並びに様々な糖鎖エピトープ結合タンパク質の特定に貢献できるものと期待される。

References

1. Karas, M., and Hillenkamp, F. (1988) Anal. Chem. **60**, 2299–2301
2. Fenn, J. B., Mann, M., Meng, C. K., Wong, S. F., and Whitehouse, C. M. (1989) Science **246**, 64–71
3. Lemoine, J., Chirat, F., and Domon, B. (1996) J. Mass Spectrom. **31**, 908–912
4. Bahr, U., Pfenninger, A., Karas, M., and Stahl, B. (1997) Anal. Chem. **69**, 4530–4535
5. Hunt, D. F., Yates, J. R., 3rd, Shabanowitz, J., Winston, S., and Hauer, C. R. (1986) Proc. Natl. Acad. Sci. U S A. **83**, 6233–6237
6. Weiskopf, A. S., Vouros, P., and Harvey, D. J. (1998) Anal. Chem. **70**, 4441–4447
7. Naven, T. J., Harvey, D. J., Brown, J., and Critchley, G. (1997) Rapid Commun. Mass Spectrom. **11**, 1681–1686
8. Solouki, T., Reinhold, B. B., Costello, C. E., O'Malley, M., Guan, S., and Marshall, A. G. (1998) Anal. Chem. **70**, 857–864
9. Chai, W., Piskarev, V., and Lawson, A. M. (2001) Anal. Chem. **73**, 651–657
10. Harvey, D. J., Bateman, R. H., Bordoli, R. S., and Tyldesley, R. (2000) Rapid Commun. Mass Spectrom. **14**, 2135–2142
11. Sagi, D., Peter-Katalinic, J., Conradt, H. S., and Nimtz, M. (2002) J. Am. Soc. Mass Spectrom. **13**, 1138–1148
12. Zhang, S., and Chelius, D. (2004) J. Biomol. Tech. **15**, 120–133
13. Karlsson, N. G., Schulz, B. L., and Packer, N. H. (2004) J. Am. Soc. Mass Spectrom. **15**, 659–672
14. Domon, B., and Costello, C. E. (1988) Glycoconj. J. **5**, 397–409
15. Meisen, I., Peter-Katalinic, J., and Muthing, J. (2003) Anal. Chem. **75**, 5719–5725
16. Xue, J., Song, L., Khaja, S. D., Locke, R. D., West, C. M., Laine, R. A., and Matta, K. L. (2004) Rapid Commun. Mass Spectrom. **18**, 1947–1955